Journal of Biomedical Optics

SPIEDigitalLibrary.org/jbo

Comprehensive data visualization for high resolution endovascular carotid arterial wall imaging

Kyle H. Y. Cheng
Cuiru Sun
Juan P. Cruz
Thomas R. Marotta
Julian Spears
Walter J. Montanera
Aman Thind
Brian Courtney
Beau A. Standish
Victor X. D. Yang

SPIE

Comprehensive data visualization for high resolution endovascular carotid arterial wall imaging

Kyle H. Y. Cheng,[a,b,c] Cuiru Sun,[a,b] Juan P. Cruz,[d] Thomas R. Marotta,[e] Julian Spears,[e] Walter J. Montanera,[e] Aman Thind,[f] Brian Courtney,[f,g] Beau A. Standish,[a,b] and Victor X. D. Yang[a,b,c,e]
[a]Biophotonics and Bioengineering Laboratory, 350 Victoria Street, Toronto, Ontario M5B 2K3, Canada
[b]Ryerson University, Department of Electrical and Computer Engineering, 350 Victoria Street, Toronto, Ontario M5B 2K3, Canada
[c]University of Toronto, Department of Electrical and Computer Engineering, 10 King's College Road, Toronto, Ontario M5S 3G4, Canada
[d]University of Toronto, Department of Medical Imaging, 150 College Street, Toronto, Ontario M5S 3E2, Canada
[e]St. Michael's Hospital, Department of Medical Imaging, 30 Bond Street, Toronto, Ontario M5B 1W8, Canada
[f]Colibri Technologies Inc., 3080 Yonge Street, Toronto, Ontario M4N 3N1, Canada
[g]Division of Cardiology, Sunnybrook Health Sciences Centre, 2075 Bayview Avenue, Toronto, Ontario M4N 3M5, Canada

Abstract. Carotid angioplasty and stenting is a minimally invasive endovascular procedure that may benefit from *in vivo* high resolution imaging for monitoring the physical placement of the stent and potential complications. The purpose of this pilot study was to evaluate the ability of optical coherence tomography to construct high resolution 2D and 3D images of stenting in porcine carotid artery. Four Yorkshire pigs were anaesthetized and catheterized. A state-of-the-art optical coherence tomography (OCT) system and an automated injector were used to obtain both healthy and stented porcine carotid artery images. Data obtained were then processed for visualization. The state-of-the-art OCT system was able to capture high resolution images of both healthy and stented carotid arteries. High quality 3D images of healthy and stented carotid arteries were constructed, clearly depicting vessel wall morphological features, stent apposition and thrombus formation over the inserted stent. The results demonstrate that OCT can be used to generate high quality 3D images of carotid arterial stents for accurate diagnosis of stent apposition and complications under appropriate imaging conditions.
[DOI: 10.1117/1.JBO.17.5.056003]

Keywords: optical coherence tomography; carotid artery; stent; thrombus.

Paper 12075P received Feb. 5, 2012; revised manuscript received Mar. 22, 2012; accepted for publication Mar. 27, 2012; published online May 4, 2012.

1 Introduction

Atherosclerosis is a disease where atheroma is deposited within the vessel wall. The atheroma is composed of variable amounts of macrophages, lipids, fibrous tissue and calcium. Depending on the composition of the lesion, the American heart Association has classified atherosclerosis from I to VI, with V and VI being considered to be high-risk lesions.[1–3] Carotid artery atherosclerosis is an important cause of ischemic stroke.[4,5] Patients with symptomatic high grade carotid stenosis benefit from revascularization.[6,7] Treatment modalities include surgical intervention, such as the resection of diseased tissue called carotid endarterectomy (CEA) or endovascular treatment such as carotid angioplasty and stenting (CAS).[8]

The coronary artery has been successfully imaged by OCT in various studies.[9] Carotid arteries, however, having large diameters and high blood flow rate, are not easily imaged with conventional Time Domain OCT systems owing to their slow imaging speed. There were only a handful of studies attempting to image the carotid artery *in vivo*.[10,11] Recently, a new state-of-the-art OCT system (Lightlab Imaging, St. Jude Medical Inc. St. Paul, Minnesota, USA) has been cleared by the FDA for clinical use in coronary imaging. With this high speed OCT system, a pilot study has been conducted on human to image stented carotid arteries after their CAS procedures.[12] Images obtained could clearly show the vessel wall anatomy and could delineate the degree of stent apposition to the vessel wall, plaque prolapse through the stent tines and the presence of a dissection flap (i.e., a tear in one of the layers of the vessel wall) or mural thrombus. These are promising results. To date, however, no animal studies on OCT imaging of carotid arteries using the state-of-the-art high speed OCT system have been conducted and experimental details have not been fully optimized. In the study described above, un-occluded saline or contrast injection was quickly ruled out because of several unsuccessful attempts and the images were obtained using two occlusion balloons in the common and external carotid arteries. Our study reported in this paper therefore, was in part to define blood clearing technique to improve OCT imaging. If a proper blood flushing protocol is not developed there are side effects such as stroke, aneurysm, and poor image quality.

In this pilot study, 4 pigs were used to optimize the OCT carotid artery imaging protocol. The overall aim of this pilot study was to validate the true feasibility of OCT carotid artery imaging using an optimized blood clearing protocol and from the data obtained, to generate 3D data sets of stent deployment to improve the accuracy as well as monitoring of stent deployment.

2 Materials and Methods

In this study, six month old 50 kg pigs ($n = 4$) were used. Each animal was ordered one week before the experiment to allow for acclimatization. All of the procedures were done with anesthesia

Address all correspondence to: Victor X. D. Yang, Ryerson University, Department of Electrical and Computer Engineering, 350 Victoria Street, Toronto, Ontario, M5B 2K3, Canada. Tel.: +416 8039320; Fax: +416 5465876; E-mail: yangv@ee.ryerson.ca

0091-3286/2012/$25.00 © 2012 SPIE

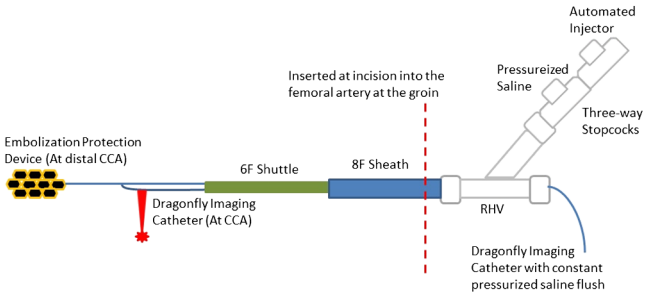

Fig. 1 Schematics of the catheter system setup.

using ketamine and continued heart rate and blood pressure monitoring. A right groin dissection to expose the femoral artery was performed and an 8F short femoral sheath was inserted. Under fluoroscopic guidance a 5F Berenstein diagnostic catheter with a 0.035 in guidewire was used to catheterize the common carotid artery (CCA). With a standard exchange maneuver a 6F long angiographic sheath (Shuttle, Cook, USA) placed in the mid CCA. A power injector was used for injection of saline or saline with contrast for blood clearance purpose during OCT. An embolization protection device (AngioGuard, Cordis, USA) was then advanced through the 6F sheath and successfully deployed in the distal CCA. The monorail OCT imaging catheter was advanced over the AngioGuard wire into the desired position. After image acquisition, the OCT catheter was removed and a monorail system vascular stent was advanced and successfully deployed. The OCT imaging probe was then re-inserted to acquire volumetric data sets of the stent after deployment. Figure 1 shows the schematics of the catheter system setup.

OCT imaging was performed by the recently FDA approved Fourier Domain OCT system with the use of the monorail imaging catheter Dragonfly (Lightlab Imaging, St. Jude Medical Inc. St. Paul, Minnesota, USA) that employs a rotary scanning

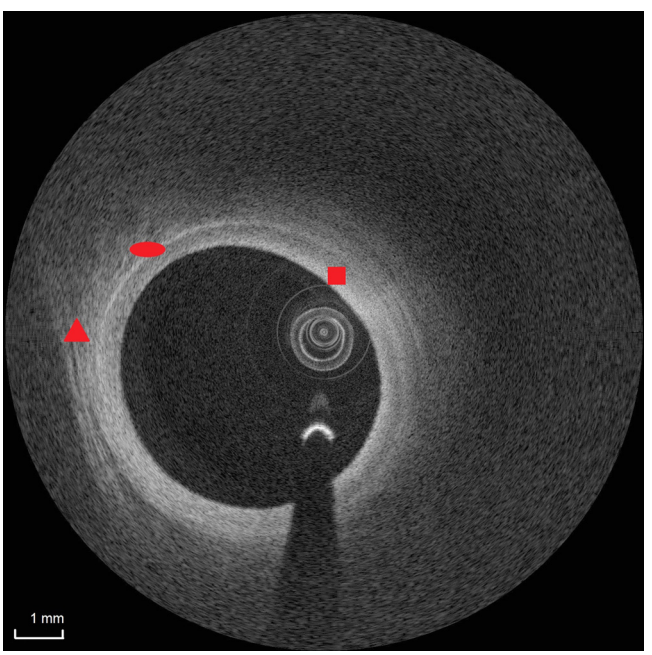

Fig. 2 EV-OCT images of normal porcine carotid artery. Square: media; ellipse: external elastic lamina; triangle: adventitia.

Fig. 3 H&E staining of normal porcine carotid artery.

mechanism in the radial direction and a pull-back scanning mechanism in the axial direction along the artery. The Fourier Domain OCT system employs a swept-source laser with center wavelength of ~1300 nm that is capable of 50000 sweeps per second, has an axial resolution of 15 μm resolution and can perform 3D rotary imaging up to 100 frames per second. An automated injector was used to inject saline or saline with contrast (Omnipaq) via a three-way stopcock to flush and clear blood during OCT imaging. Different injection schemes were tested to ensure optimized image quality for a typical 30 mm carotid plaque length.

The data obtained were then processed, where visual comparison between data sets would allow for the determination of the best injection scheme. Due to the pulsation of the heart beat cycle and the finite duration of the pullback mechanism, the position of the carotid artery would fluctuate between each frame. The frames can be co-registered by rigid translation using cross correlation analysis between each frame.[13] After the frames were co-registered, the data was imported into a

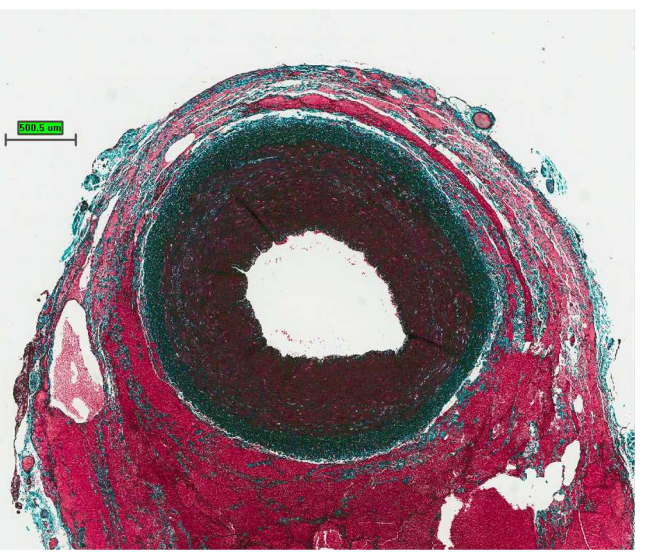

Fig. 4 Elastin trichrome staining of normal porcine carotid artery.

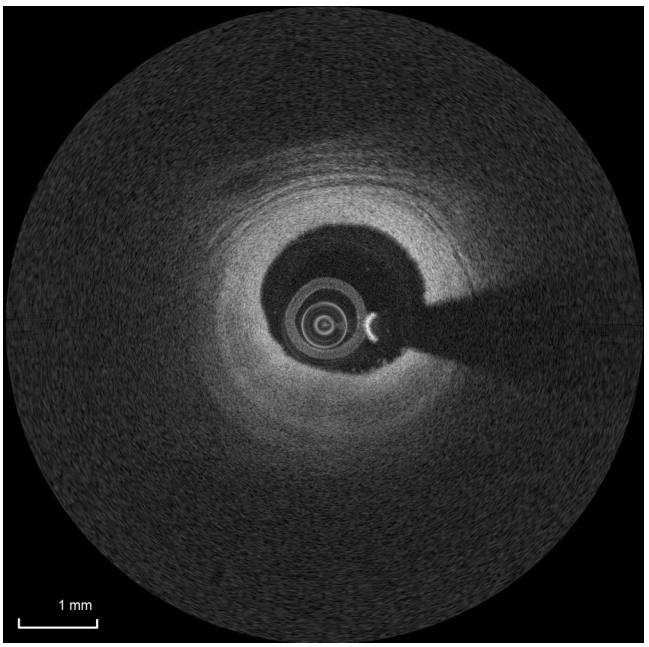

Fig. 5 EV-OCT image of porcine carotid artery undergoing vasospasm.

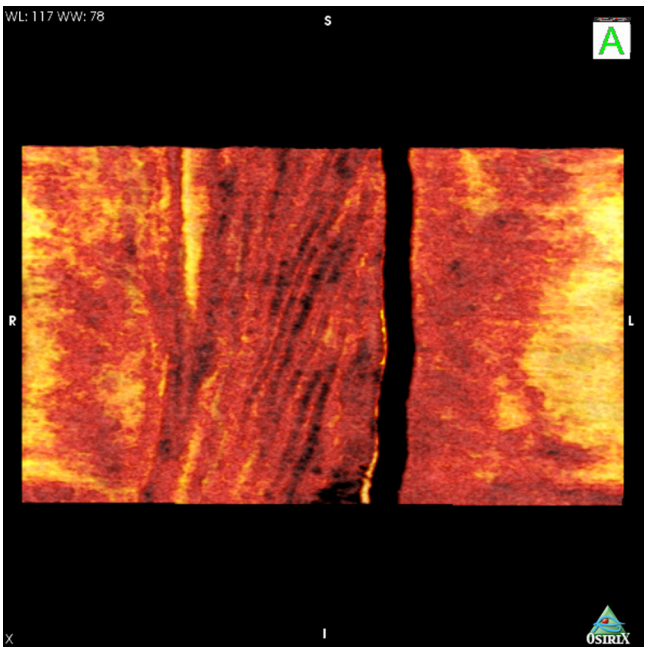

Fig. 7 Flattened view of porcine carotid artery adventitia.

DICOM image viewer (OsiriX, The OsiriX Foundation, Geneva, Switzerland), to construct a 3D view of the carotid artery with stenting.

The study was approved by Animal Care Committee of Saint Michael's Hospital, Toronto, Ontario, Canada. (Protocol ID: ACC 307) and follows the guidelines of Canada Council on Animal Care's (CCAC) Ethics of Animal Investigation.

3 Results

Different imaging catheter pullback speed and contrast/saline injection rate were tested. In general, no noticeable difference was observed between pure saline and saline with contrast and pullback speed equal to or below 6 mm/s and contrast/saline injection rate of $5 \sim 8$ cc/s would give the best results. Therefore, normal carotid artery imaging was optimized at ~6 cc/s contrast/saline injection rate at a pullback speed of ~5 mm/s. The consequence of using higher injection speed or pullback rate will be presented in discussion section.

Figure 2 shows the OCT image of normal porcine carotid artery. Figures 3 and 4 show a representative hematoxylin and eosin (H&E) staining and elastin trichrome staining of the porcine carotid artery wall, respectively. The OCT image clearly delineates the media, the external elastic lamina and the adventitia. In a recent study by our group, it was also

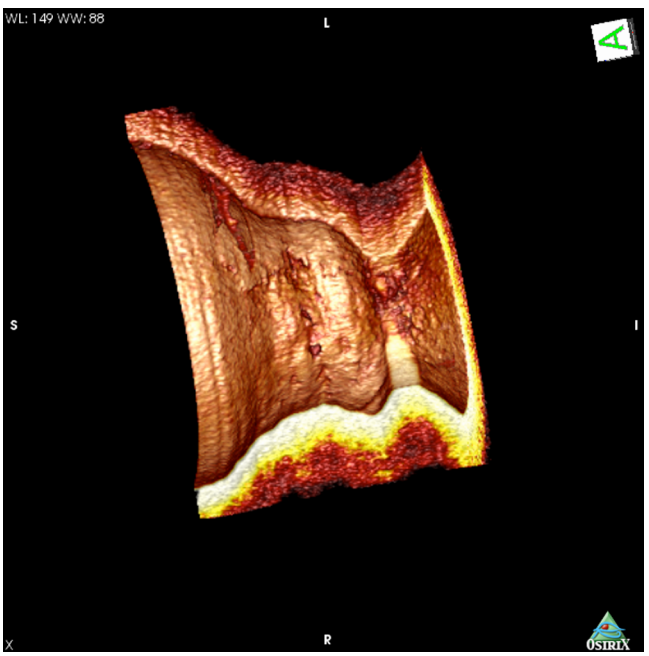

Fig. 6 3D view of vasospasm.

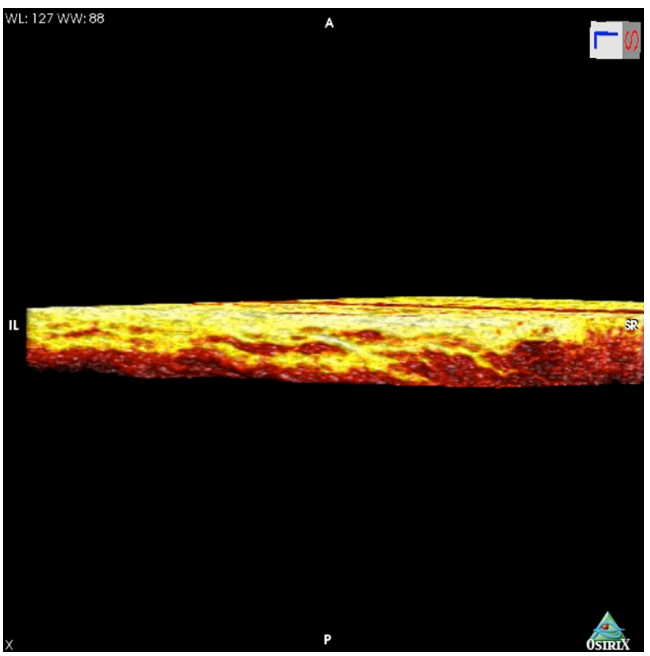

Fig. 8 Side view of flattened adventitia.

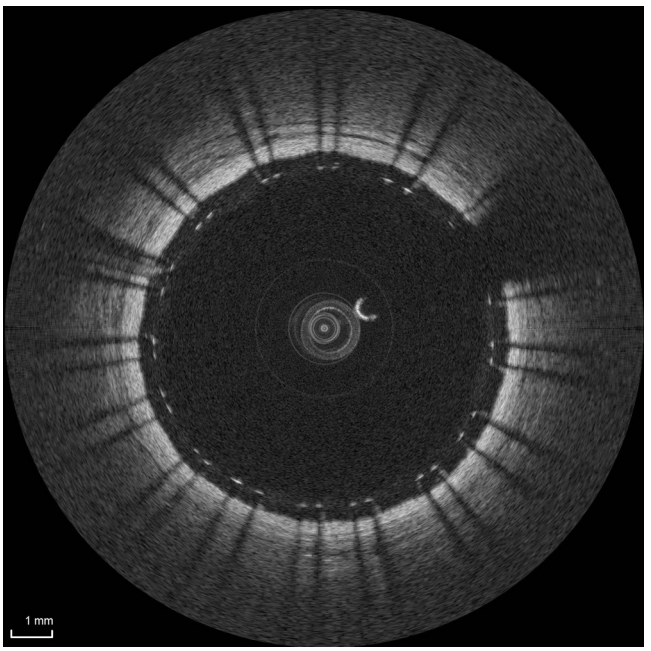

Fig. 9 EV-OCT image of stented porcine carotid artery.

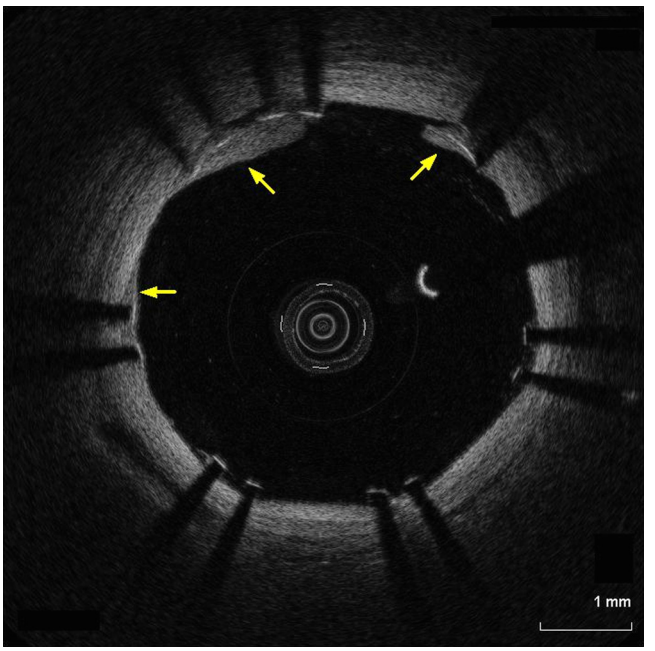

Fig. 11 Stented porcine carotid artery with clots formed over the stent, arrows indicate clot locations.

demonstrated that EV-OCT can potentially detect vasa vasorum *in vivo*.[14] Figure 5 shows a representative image of vasospasm of porcine carotid artery. A 3D reconstruction of the spasm segment is shown in Fig. 6. Note that the EV-OCT provides 2D cross-section views of the endovascular structures of pig carotid artery, where the data obtained by the pullback can also help form 3D rendering visualization of the carotid artery, allowing physicians to evaluate the size, morphology and distinctive features of the vessel wall for clearer and more efficient diagnosis. To demonstrate the rich information contained in a 3D data set of EV-OCT data, Fig. 7 shows the 3D rendering view of a flattened adventitia layer of the porcine carotid artery obtained by vessel wall surface detection and alignment. From the flattened view, a distinctive network of channels is very clearly present in the image, which otherwise would not be visible in a cross-sectional rotary view of carotid artery EV-OCT. Figure 8 also shows the side view of the flattened adventitia.

Upon the optimized protocol for EV-OCT imaging, CAS was performed using standard carotid artery stents. Figure 9 shows a representative stent image using pullback speed of 5 mm/s and

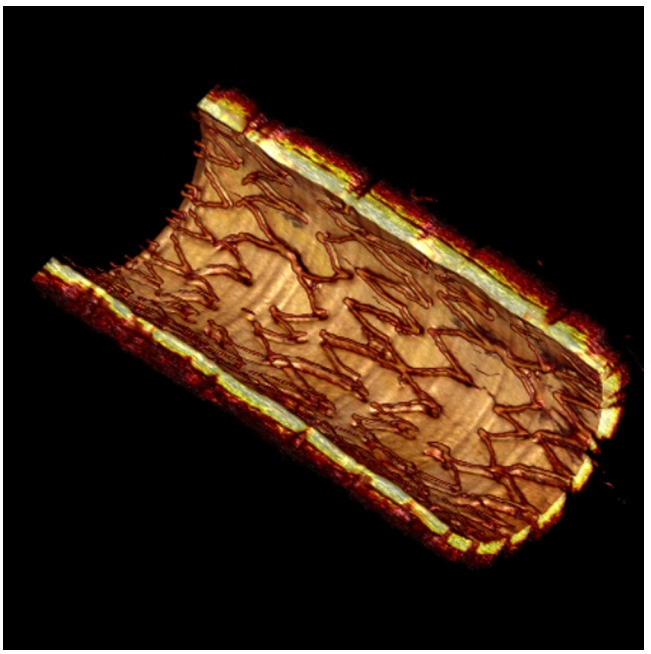

Fig. 10 3D rendering of properly stented pig carotid artery (Video 1, QuickTime, MOV, 2.12 MB). [URL: http://dx.doi.org/10.1117/1.JBO.17.5.XXXXXX.1]

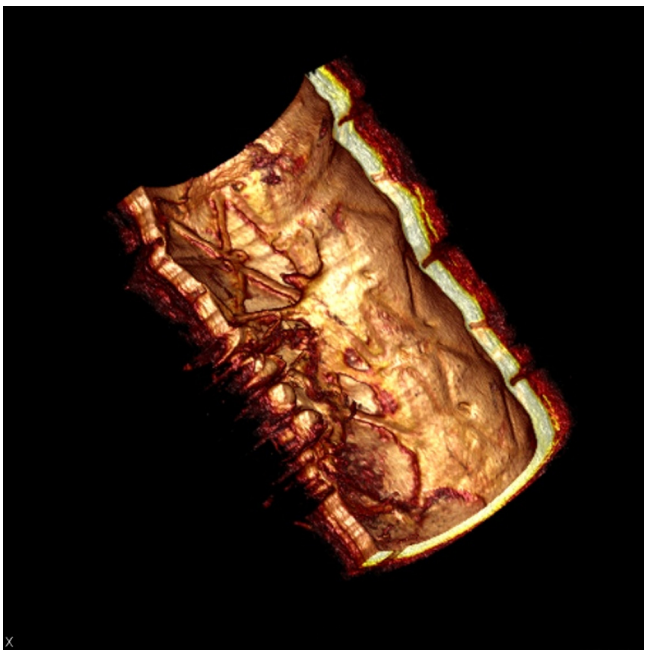

Fig. 12 3D rendering of stented porcine carotid artery with blood clots forming over the stent (Video 2, QuickTime, MOV, 1.46 MB). [URL: http://dx.doi.org/10.1117/1.JBO.17.5.XXXXXX.2]

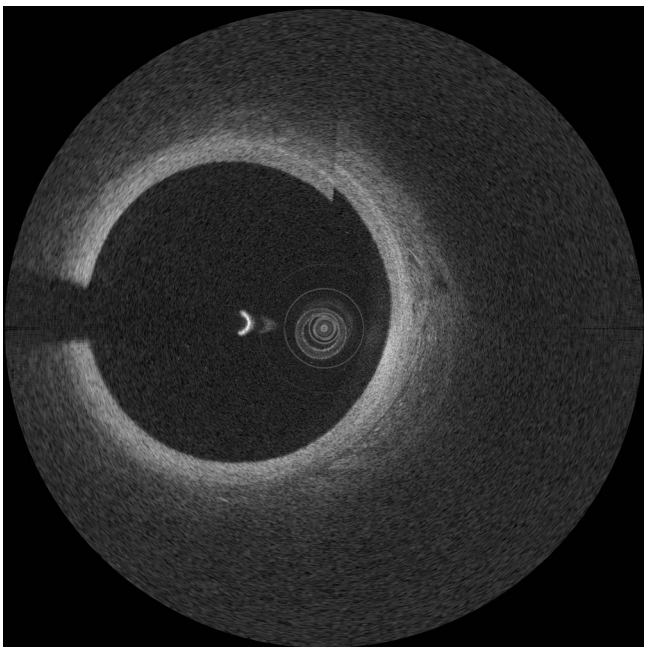

Fig. 13 Image jittering resulting from excessive contrast injection or high imaging catheter pull-back speed.

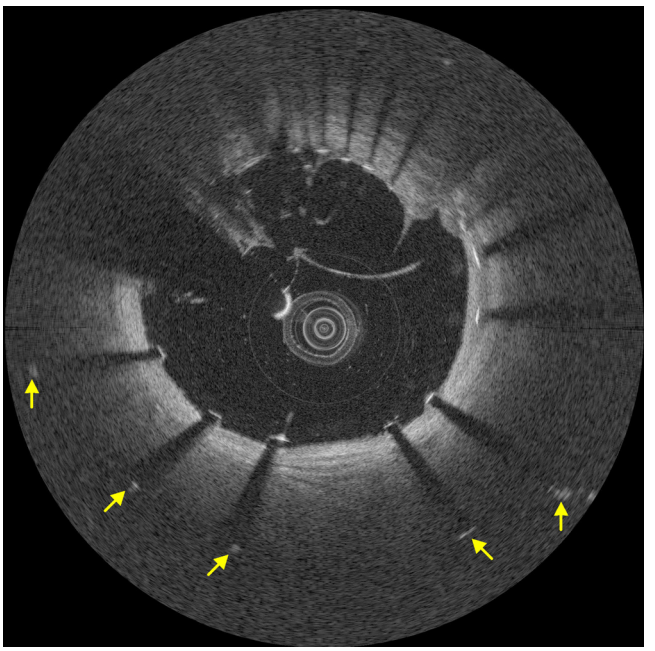

Fig. 14 EV-OCT image artifacts caused by double reflection. Notice that many stent strut locations are falsified (indicated by arrows), with some displayed inside the lumen and some being displayed all the way into the adventitia.

flush injection rate of 5 cc/s. From the image, the stent apposition can be clearly discerned. The image sequence was used to construct a 3D rendering of the stent. A representative rendering is shown in Fig. 10 (fly through video). Not only can a 3D rendering of OCT images visualize stent apposition, but it can also visualize complications such as blood clot and fibrin formation over the stent. A representative image is shown in Fig. 11, with a representative 3D rendering shown in Fig. 12 (fly through video).

4 Discussion

Atherosclerotic plaque characterization in the coronary arteries has been extensively studied with intravascular ultrasound, and OCT has emerged more recently as a valuable tool in predicting the risk of potential rupture.[15,16] On the other hand, carotid plaques have been mainly studied with ultrasound, computed tomography angiography or MRI.[17–19] OCT has the potential to expand our understanding of the individual risk of stroke from a carotid plaque.

During the experiments, the pullback speed of the imaging catheter was limited to 6 mm/s and the injection rate of the saline/contrast was limited to 5 cc/s. Higher contrast injection rate would induce high frequency vibration of the imaging catheter and would result in image jittering as shown in Fig. 13. However, there are image artifacts, most noticeably double reflection that one must beware of (an example is given in Fig. 14). These artifacts should not be misinterpreted as features as this can possibly lead to false-positives.

From Fig. 2, the image clearly demonstrates that EV-OCT is capable of providing high resolution images in high blood flow vessels such as the carotid artery. This can be further confirmed by the H&E and elastin trichrome staining histology in Figs. 3 and 4. The media, external elastic lamina and the adventitia are well correlated with histology. An example of vasospasm, which is a focal reduction in the vessel lumen secondary to contraction of the vessel wall smooth muscle, was imaged by EV-OCT and shown in Fig. 5. In the wake of rapidly advancing computer speeds and display technologies, manipulation of EV-OCT data in the domain of 3D visualization can prove to be valuable in evaluation of conditions in the carotid artery. Figure 6 shows the 3D rendering of the vasospasm segment. This may allow clinicians to fully appreciate the extent and nature of the luminal narrowing. Further manipulation of EV-OCT data can also bring out interesting information. In Fig. 7, the flattened view of the carotid artery adventitia shows distinct channels in half of its surface area. These channels are suspected to be nerves since the water content in peripheral nerves are high and as such have a low back scattering coefficient. Therefore, the nerves would appear as dark channels. Figure 8 shows the side view of the adventitia, in contrast to the view in Fig. 7, the other half of the area of the adventitia is comprised mainly of laminar structures. Therefore EV-OCT has the potential to further our understanding on the physiological responses of the cardiovascular system in correlation to its anatomical features.

In order to enhance diagnostic efficiency and evaluate the overall apposition of the carotid stent, a 3D view of a stented vessel is indispensable. Tearney et al. have previously accomplished a considerable body of research on this aspect in a previous study using OCT systems.[20] However, for carotid artery, a faster and more robust OCT system is needed for 3D reconstructions due to the high blood flow rate and larger vessel diameter. With the Fourier Domain OCT system, complete 3D views of the stent after CAS using intensity thresholding were obtained (Fig. 10). The degree of apposition of the stent to the vessel wall is clearly depicted. This was due to the fact that metal stents pose a much lower probability of direct back reflection of light into the imaging catheter (due to surface curvature) than the vessel lumen surface. Thus when mapping to colors corresponding to lower intensity values, they can be clearly distinguished from the vessel wall tissues. Not only can the stent be clearly visualized, but also stent associated bland thrombus formation can be

clearly identified (Fig. 12). This is possible as blood and thrombus are highly scattering media.

The ability of EV-OCT to image the carotid artery and to generate 3D visualization of the stented artery was demonstrated in this study. The optimal flushing and imaging protocols were also developed. Further study should be carried out in pig models of different stages of carotid atherosclerosis to generate an atlas to provide a complete description of the disease progress, as well as on stenting in diseased artery to evaluate possible complications of CAS.

5 Conclusion

In this study, endovascular carotid imaging protocols were optimized to obtain suitable image quality without flow occlusion. EV-OCT was also demonstrated to be capable of generating high-resolution images of both healthy and stented pig carotid arteries. Pathologically relevant features were correlated to identify EV-OCT biologically relevant tissue structures. Furthermore, 3D rendering of stented carotid arteries were generated, clearly visualizing stent apposition. This technique has the potential to provide a higher level of accuracy for the evaluation of carotid stent deployment and its associated immediate complications.

Acknowledgments

The authors acknowledge funding support from NSERC, ERA, CIHR and Ryerson University. We would like to thank the animal surgical technicians, Ms. Lauren McKeeman and Ms. Danielle Gifford in the animal vivarium of Saint Michael's Hospital for their grateful help on the animal experiments.

References

1. H. C. Stary et al., "A definition of the intima of human arteries and of its atherosclerosis-prone regions. A report from the Committee on Vascular Lesions of the Council on Arteriosclerosis, American Heart Association," *Circulation* **85**(1), 391–405 (1992).
2. H. C. Stary et al., "A definition of advanced types of atherosclerotic lesions and a histological classification of atherosclerosis," *Circulation* **92**(5), 1355–1374 (1995).
3. H. C. Stary et al., "A definition of initial fatty streak, and intermediate lesions of atherosclerosis. A report from the Committee on Vascular Lesions of the Council on Arteriosclerosis, American Heart Association," *Arterioscler. Thromb. Vasc. Biol.* **14**(5), 840–856 (1994).
4. W. G. Members et al., "Heart disease and stroke statistics—2010 update: A report from the American Heart Association," *Circulation* **121**(7), e46–e215 (2010).
5. S. Kinlay, "Changes in stroke epidemiology, prevention and treatment," *Circulation* **124**(19), e494–e496 (2011).
6. H. J. M. Barnett et al., "Benefit of carotid endarterectomy in patients with symptomatic moderate or severe stenosis," *N. Engl. J. Med.* **339**(20), 1415–1425 (1998).
7. North American Symptomatic Carotid Endarterectomy Trial Collaborators, "Beneficial effect of carotid endarterectomy in symptomatic patients with high-grade carotid stenosis," *N. Engl. J. Med.* **325**(7), 445–453 (1991).
8. T. G. Brott et al., "Stenting versus endarterectomy for treatment of carotid-artery stenosis," *N. Engl. J. Med.* **363**(1), 11–23 (2010).
9. A. F. Low et al., "Technology insight: optical coherence tomography—current status and future development," *Nat. Clin. Pract. Cardiovasc. Med.* **3**(3), 154–162 (2006).
10. M. S. Mathews et al., "Neuroendovascular optical coherence tomography imaging and histological analysis," *Neurosurgery* **69**(2), 430–439 (2011).
11. S. Yoshimura et al., "OCT of human carotid arterial plaques," *J. Am. Coll. Cardiol. Img.* **4**(4), 432–436 (2011).
12. B. Reimers et al., "Preliminary experience with optical coherence tomography imaging to evaluate carotid artery stents: safety, feasibility and techniques," *EuroIntervention* **7**(1), 98–105 (2011).
13. M. Guizar-Sicairos, S. T. Thurman, and J. R. Fienup, "Efficient subpixel image registration algorithms," *Opt. Lett.* **33**(2), 156–158 (2008).
14. K. H. Y. Cheng et al., "Endovascular optical coherence tomography intensity kurtosis: visualization of vasa vasorum in porcine carotid artery," *Biomed. Opt. Express* **3**(3), 388–399 (2012).
15. A. Nair et al., "Coronary plaque classification with intravascular ultrasound radiofrequency data analysis," *Circulation* **106**(17), 2200–2206 (2002).
16. R. Puri, M. I. Worthley, and S. J. Nicholls, "Intravascular imaging of vulnerable coronary plaque: current and future concepts," *Nat. Rev. Cardiol.* **8**(3), 131–139 (2011).
17. J. F. Polak, "Carotid ultrasound," *Radiol. Clin. North Am.* **39**(3), 569–589 (2001).
18. B. A. Wasserman, "Advanced contrast-enhanced MRI for looking beyond the lumen to predict stroke: building a risk profile for carotid plaque," *Stroke* **41**(10 Suppl), S12–S16 (2010).
19. Y. Watanabe and M. Nagayama, "MR plaque imaging of the carotid artery," *Neuroradiology* **52**(4), 253–274 (2010).
20. G. J. Tearney et al., "Three-dimensional coronary artery microscopy by intracoronary optical frequency domain imaging," *J. Am. Coll. Cardiol. Img.* **1**(6), 752–761 (2008).